

Okoe, M., Alam, S. S. & Jianu, R. (2014). A Gaze-enabled Graph Visualization to Improve Graph Reading Tasks. *Computer Graphics Forum*, 33(3), pp. 251-260. doi: 10.1111/cgf.12381



**CITY UNIVERSITY  
LONDON**

[City Research Online](#)

**Original citation:** Okoe, M., Alam, S. S. & Jianu, R. (2014). A Gaze-enabled Graph Visualization to Improve Graph Reading Tasks. *Computer Graphics Forum*, 33(3), pp. 251-260. doi: 10.1111/cgf.12381

**Permanent City Research Online URL:** <http://openaccess.city.ac.uk/15378/>

### **Copyright & reuse**

City University London has developed City Research Online so that its users may access the research outputs of City University London's staff. Copyright © and Moral Rights for this paper are retained by the individual author(s) and/ or other copyright holders. All material in City Research Online is checked for eligibility for copyright before being made available in the live archive. URLs from City Research Online may be freely distributed and linked to from other web pages.

### **Versions of research**

The version in City Research Online may differ from the final published version. Users are advised to check the Permanent City Research Online URL above for the status of the paper.

### **Enquiries**

If you have any enquiries about any aspect of City Research Online, or if you wish to make contact with the author(s) of this paper, please email the team at [publications@city.ac.uk](mailto:publications@city.ac.uk).

# A Gaze-enabled Graph Visualization to improve graph reading tasks

Submission 235

---

## Abstract

*Performing typical network tasks such as node scanning and path tracing can be difficult in large and dense graphs. To alleviate this problem we use eye-tracking as an interactive input to detect tasks that users intend to perform and then produce unobtrusive visual changes that support these tasks. First, we introduce a novel fovea based filtering that dims out edges with endpoints far removed from a users view focus. Second, we highlight edges that are being traced at any given moment or have been the focus of recent attention. Third, we track recently viewed nodes and increase the saliency of their neighborhoods. All visual responses are unobtrusive and easily ignored to avoid unintentional distraction and to account for the imprecise and low-resolution nature of eye-tracking. We also introduce a novel gaze-correction approach that relies on knowledge about the network layout to reduce eye-tracking error. Finally, we present results from a controlled user study showing that our methods led to a statistically significant accuracy improvement in one of two network tasks and that our gaze-correction algorithm enables more accurate eye-tracking interaction.*

---

**Keywords:** Eye tracking, gaze contingent graph visualization.

## 1. Introduction

Network analysis plays an important part in domains such as neuroscience [BS09], genomics and proteomics [CCNS08], transportation [KT06], software engineering [GN00], social sciences [BMBL09], or intelligence analysis [CGM04]. Interaction is instrumental in allowing users to weed through the scale, complexity, and clutter inherent to visualizations of real-life networks. Here we explore the use of eye tracking as an interactive input to detect users' intentions and support them by slight changes in the visualization. The use of eye tracking as an input has been explored in the human computer interaction (HCI) community [Duc02], but it has not yet been explored in the area of network visualization.

Specifically, we introduce three types of interactions. First, we reduce clutter by using a novel fovea-based filtering that dims edges that pass through the

user's view focus but have their endpoints far outside of the user's fovea. Second, we increase the saliency of edges as they are visually traced by the user at any given moment or have been the focus of frequent recent tracings. Third, we keep track of nodes that were recently viewed and increase the salience of their neighborhood. All visual responses are gradual, incremental rather than binary, and visually subtle.

Thus, by design, our interactions are gaze-contingent [Duc02]. This means gaze coordinates are used to infer users' task intentions and the visualization is changed to support these tasks as unobtrusively as possible to minimize distraction and account for errors of interpretation. This approach also relates to attentive interfaces [Duc02, Sel04] and multimodal interfaces [Ovi03] but contrasts with early HCI efforts to use eye-tracking in ways analogue to manual pointing and clicking. Merely connecting eye-tracking input to otherwise conventional network interactions is limited due to the particularities of eye-movements and eye-tracking technology. Specifically, as noted by [ZMI99], the eyes are not a control organ, eye-tracking input is generally low resolution and inaccurate, and the ab-

sence of a trigger analogue to a mouse click is difficult to compensate [Jac90].

An additional contribution of our work is a gaze-correction algorithm that uses knowledge of the visualization layout to reduce eye-tracking error. Faulty or insufficient calibration sometimes leads to localized screen regions in which gaze-coordinates are offset from the users true viewing point. Our algorithm relies on the known visual positioning of nodes on the screen to detect which nodes users are likely to be looking at.

In a controlled within-subject user study with twelve participants, we evaluated the performance of our gaze-enabled network visualization. We asked participants to perform two types of tasks: (i) identify whether there is a direct connection between two nodes; and (ii) identify the shortest path between two nodes. In a third task designed to evaluate the efficiency of our gaze correction algorithm, users were asked to select as many nodes as possible in a given time interval by looking at them, with and without gaze correction. Our results were statistically significant ( $p = 0.02$ ) and showed a 30% improvement in the direct connection task, were not significant in the path task, and showed a significant ( $p = 0.01$ ) 25% improvement in the node selection task.

## 2. Related Work

The fovea, a small area in the center of the retina, is responsible for our high resolution vision. The rest of our field of view is low resolution and defined as peripheral. The illusion of complete high definition vision is created by an unconscious scanning process: the fovea performs quick translations, called saccades, during which vision is temporarily blinded, between short moments of focus, called fixations. Eye-tracking technology allows us to locate users' points of gaze [WM87, Jac91].

Most often, gaze tracing is used for data collection in offline, post hoc analyses of human visual perception [Duc07]. Examples of eye-tracking facilitated analyses span a broad range of domains including cognitive science, psychology, education, marketing, and interface design. In data visualization, eye-tracking has traditionally been used in post hoc analyses of visualization perception and interpretation. For example, Huang et al. [HEH08] or Pohl et al. [PSD09] use eye-tracking in the context of understanding network visualization use.

The appeal of the eye's speed led human computer interaction researchers to also explore gaze as an actuator input in ways analogue to manual input (e.g. mouse). This approach has met with limited success due to several reasons. First, while very

fast, gaze-input comes with disadvantages such as low accuracy, jitter, drift, offsets, and calibration needs [Duc07, JK03, TJ00, KPW07]. Second, finding a gaze equivalent of a trigger command is not trivial and leads to the Midas touch phenomenon - the inability of the interface to reliably distinguish between looking and controlling [Jac91]. Ultimately, the duration of a fixation, or dwell time, has been established as the most effective way to trigger commands [WM87, Jac91]. However, low dwell thresholds amplify the Midas touch problem by triggering commands inadvertently, while high dwell thresholds offset the speed advantage of gaze input.

The current consensus is that eyes are not control organs and should not be treated as such [ZMI99]. Instead, Jacob proposed that interfaces should use gaze as an indicator of user intention and should react with gradual, unobtrusive changes [Jac91, JK03]. This view is formalized within the concept of attentive interfaces [ADS05, Ver02, VSCM06, VS08, HMR05, RHN\*03] which "(a) monitor user behavior, (b) model user goals and interests, (c) anticipate user needs, (d) provide users with information, and (e) interact with users" [MMC\*00]. The research described here aligns with this paradigm and also drew inspiration from work in gaze-contingent rendering [OHM\*04, DÇ07, HDO03], where scenes are drawn in high resolution in foveated screen areas and with lower quality in regions outside of the user's focus.

To the best of our knowledge, in visualization in general and network visualization in particular, eye tracking has only been used in a diagnostic role. Given the unavoidable connection between eyes and data visualization, the fact that people's gazes are linked to tasks they are performing [YR67], and that eye-tracking is on its way to becoming a component of regular work stations [Duc07, JK03, LBP06], we hypothesize that visualization research can benefit from exploring use of eye-tracking as an input channel. The results presented here demonstrate this approach and introduce concrete techniques and algorithms.

## 3. Implementation

To develop a gaze responsive network visualization, we focused our methods on two issues: improving gaze accuracy and providing interactive visual responses. The interactive responses are: (i) a novel fovea based filtering that dims out edges with endpoints far removed from a user's view focus; (ii) highlighting edges that are being traced at any given moment or have been the focus of recent attention; (iii) tracking recently viewed nodes and increasing the saliency of their neighborhoods. We detail these techniques in the following sections.

### 3.1. Gaze-correction

Due to poor or insufficient calibration offsets, reported eye-tracking coordinates are sometimes slightly offset from true gaze positions in some screen areas. We hypothesized we can alleviate this problem by leveraging the known network layout, and on the assumptions that users rarely stare at blank screen space and that long fixations correspond to node fixations. Conceptually, we matched offset-vectors between subsequent long fixations (200-300ms) to offset-vectors between nodes lying close to these fixations (Fig. 1) to identify offsets between reported coordinates and nodes that were likely the target of the users attention. We aggregate these offsets over time, gradually constructing and adjusting an offset map over the screen space. This offset map is then used to correct all incoming gaze coordinates. In (Fig. 2), we show a depiction of a gaze correction. The magnitude of vectors in the offset map is displayed as a red heatmap, while the centers of the blue and red circles represent corrected gaze and raw gaze respectively.

Concretely, our implementation works as follows. We maintain a list of the last three fixations, as they are delivered by the eye-tracker API. Whenever this list changes we do the following. For each of the three fixations we find the closest three network nodes and we construct nine possible combinations. For each combination we compute a score that averages two components: proximity of the gazes to their corresponding nodes; and differences between vectors constructed between three pairs of gaze points and the three pairs of corresponding nodes. We then choose the best scored configuration, and if it is below a threshold, we consider that the current three fixations match those three nodes. This allows us to compute offsets between reported fixation coordinates and likely true coordinates.

Finally, we integrate the currently computed offset into the existing offset map. This map is essentially a partitioning of the screen space into cells of 10x10 pixels, where each cell contains a two-dimensional vector representing the offset that should be applied to any subsequent gaze landing in that cell. To integrate an offset vector into the map we combine (e.g., weighted average) the current offset vector with the vector currently stored in the map. We also do this for cells neighboring that where the gaze landed, albeit with a decreasing contribution into the current score (e.g., less weight), depending on how far removed the neighboring cell is from the reported or center cell.

Correction happens in screen space rather than visualization space and as such the computed offset map is bounded in size. This means it can be computed relatively quickly and then adjusted on the fly as users

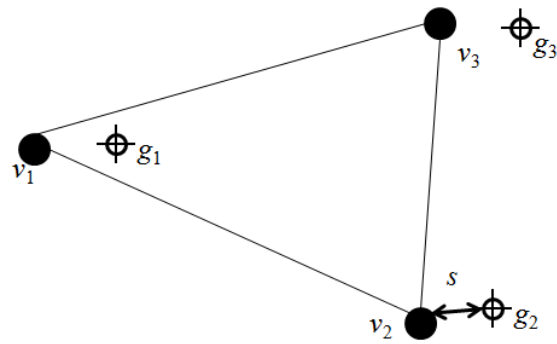


**Figure 1:** Correcting the gaze input: Even though fixations  $g_1, g_2, g_3$  are not exactly over graph vertices  $v_1, v_2, v_3$  their relative position matches that of the proximal graph vertices. We therefore conclude that  $g_1, g_2, g_3$  were fixations on the graph vertices  $v_1, v_2, v_3$ .

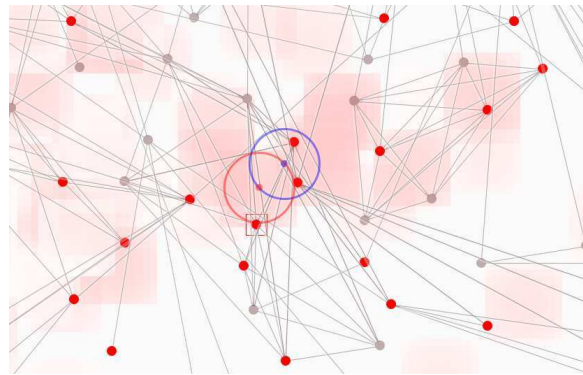


**Figure 2:** Gaze correction in our system. The blue circle represents the corrected gaze while the red one matches the raw gaze sample. Red indicates regions with high offsets.

interact with the visualization and viewing conditions change.

We note that in a sense this approach is similar to work by Salvucci et al. [Sal99, SA00] who use Markov and Bayesian models to predict gaze targets based on probable behavior, to that of MacKenzie and Zhang [MZ08] who use letter and word prediction to improve their eye-typing system, and finally to work interpreting fixations as part of gaze gestures [DS07, DDLS07].

### 3.2. Gaze-enabled network interactions

We implemented three types of interactions. The next three sub-sections describe a series of node and edge scores that are computed from gaze data. The fourth sub-section describes how these scores are combined and used during rendering to create visual responses.

The last sub-section discusses a few implementation details that apply to all interactions.

### 3.2.1. Gaze-enabled filtering

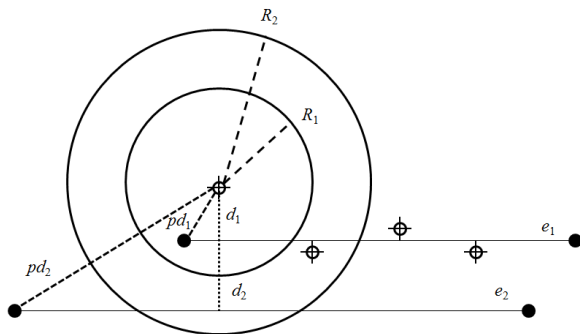


Figure 3: Foveated edge filtering.

Gaze-enabled edge filtering aims to dim edges that pass through the user’s fovea but have both endpoints far removed from it. To achieve this, given a current gaze point, we compute filtering scores ( $S_{ef}$ ) for all edges according to the diagram in Figure 3 and using Formula 1. Specifically, we use two circles centered at the user’s focus point to create a gradual transition between areas in which the filtering is applied (foveated region, inner circle) and where it is not (peripheral region, outside the outer circle). Current edge scores are combined with previous scores to ensure gradual changes in this measure. Finally,  $S_{ef}$  is combined with other saliency measures and used to render edges, as will be described in section 3.2.4.

$$S_{\text{flt}} = f(pd) + (1 - f(pd)) \times \min\left(1, \frac{d}{R_2}\right) \quad (1)$$

$$\text{where } f(pd) = 1 - \frac{pd - R_1}{R_2 - R_1}$$

### 3.2.2. Detecting viewed edges

We also aim to detect edges that are viewed as users are tracing them and increase their saliency. To this end we compute edge viewing scores ( $S_{ev}$ ) for all edges.

We first divide edges into segments of equal lengths. A score is maintained for segment endpoints to indicate whether recent gazes landed nearby. Each gaze sample landing close to an edge segment endpoint will increase the endpoint’s score by a factor inversely proportional to the distance between the gaze and the endpoint. At the same time all scores are gradually decreased each time a new gaze is processed.

These segment endpoint scores are combined into

a total edge score as follows. A bar is extended in both directions of an endpoint with non-zero score (Figure 4). The bar’s length is directly proportional with the magnitude of the score. All bar lengths of an edge are then added together, divided by a constant, in our case 500, and capped to 1. This step ensures edge scores between 0 and 1 and gives preference to edges close to or longer than 500 pixels.



Figure 4: Computing edge score segment bars.

An improvement was introduced to account for a behavior observed during testing. People seemed to require shorter fixations and longer saccades when tracing edges that were fairly isolated or travelling through empty space, but required longer fixations with shorter saccades between them when tracing edges in dense areas. To account for this, we compute a density score for each segment endpoint by adding up the number of other endpoints that lie within a certain distance from it. We use this density score to extend longer bars from low density endpoints and shorter bars from high density endpoints. This ensures that we easily detect views of isolated edges yet at the same time reduce false positives in dense areas where two random fixations could easily match an edge.

Two types of edge viewing scores are computed using this methodology. The first is a short-term score ( $S_{ev}$ ) that captures edges that are currently viewed. This score can change between its minimum and maximum values within a few hundred milliseconds. The second is a long-term score ( $S'_{ev}$ ) that captures edges of interest, those that have been viewed repeatedly in the last several seconds. We use the first score to increase or decrease the value of the second score by a constant that depends on the desired life-span of the second score.

### 3.2.3. Detecting sub-networks of interest

Highlighting sub-networks of interest aims to make node neighborhoods that are of current interest more salient. To achieve this we first compute an interest score for each node in a way analogue to edge segment endpoint scores: if a user’s gaze lingers close to a node, its score will be increased by a factor inversely proportional to the distance between the gaze and the node. As in the case of edges, we decay all node scores each time a new gaze is processed.

Once node scores are computed we diffuse them across their neighborhoods. For example, for a current gaze fixation  $g$ , the closest  $m$  vertices  $\{v_1, v_2, \dots, v_m\}$

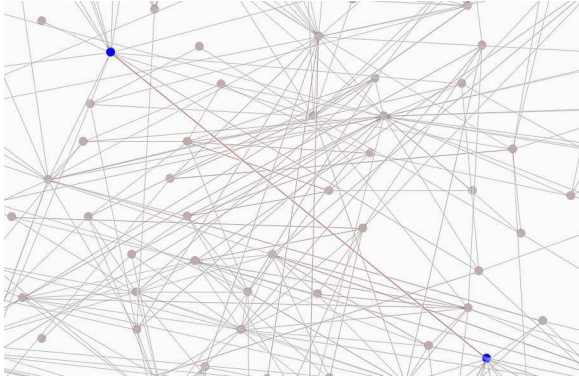


Figure 5: Highlighting of a viewed edge.

get a particular score  $s$ . The next level of adjacent vertices  $\{v_{i_1}, v_{i_2}, \dots, v_{i_m}\}$  for each  $v_i \in \{v_1, v_2, \dots, v_m\}$  gets a score of  $s/f$  where  $f$  is a dividing factor. We continue this diffusion process until vertices in level  $n$  receive score  $\frac{s}{f^{n-1}} < t$  where  $t$  is a threshold. In our implementation we have kept  $m = 3$  and  $f = 4$ . Similarly to edges scores, we keep two scores for each node, a short term score  $S_v$  computed as described above and a long term score  $S'_v$  that is computed from  $S_v$ .

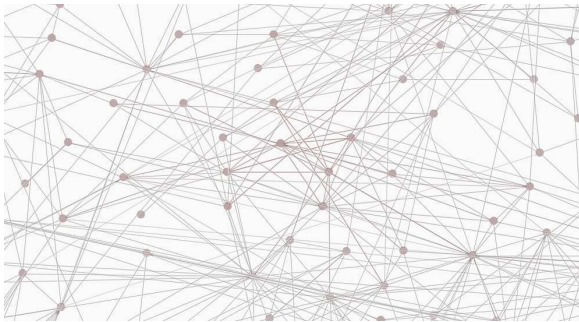


Figure 6: Highlighting a sub-network of interest.

### 3.2.4. Rendering

We described several types of scores computed for nodes and edges. Upon rendering we combine these scores and link them to visual properties such as color and alpha blending. In our implementation we have used the mapping described below. However, we note that other mappings can be explored as long as they are gradual and unobtrusive.

When drawing nodes, the previously described node scores  $S_v$  and  $S'_v$  are factored into the node's color and opacity. To compute node color we used formula 2 while for opacity we used formula 3. The four constants determine the base color for unviewed nodes,

the saliency for viewed nodes, and weight of each score into the visual response. The values chosen in our evaluated implementation, given color components between 0 and 255, were  $C_1 = 50, C_2 = 30, C_3 = 90, C_4 = 120$ .

$$\begin{aligned} \text{Red}(v) &= C_1 + S_v \times C_2 + S'_v \times C_3 \\ \text{Green}(v) &= C_1 \\ \text{Blue}(v) &= C_1 \end{aligned} \quad (2)$$

$$\text{Alpha}_v = C_1 + S_v \times C_2 + S'_v \times C_4 \quad (3)$$

Similarly, when drawing edges we also varied opacity and the red color component to highlight interesting edges, as shown in formulas 4, 5, 6. Moreover, we rendered edges in two layers: a short-term layer that highlights edges currently viewed and a long-term layer to highlight edges that have been of interest in the last several seconds or more.

$$\begin{aligned} \text{Red}(u, v) &= C_5 + C_6 \times S_{ev} \\ &\quad + C_7 \times S_{ev, long} \\ &\quad + C_8 \times \frac{(S'_u + S'_v)}{2} \end{aligned} \quad (4)$$

$$\begin{aligned} \text{Green}(u, v) &= C_5 \\ \text{Blue}(u, v) &= C_5 \end{aligned}$$

$$\begin{aligned} \text{Alpha}(u, v) &= S_{ef} \times (C_9 + C_{10} \times S_{ev}) \\ &\quad + C_{11} \times (1 - S_{ef}) \times S_{ev} \end{aligned} \quad (5)$$

$$\begin{aligned} \text{Alpha}'(u, v) &= S_{ef} \times (C_{12} \times S'_{ev} + C_{13} \times \frac{(S'_u + S'_v)}{2}) \\ &\quad + C_{14} \times (1 - S_{ef}) \\ &\quad \times (C_{12} \times S'_{ev} + C_{13} \times \frac{(S'_u + S'_v)}{2}) \end{aligned} \quad (6)$$

In the color computation,  $C_5$  indicates the base component of edges (125 in our implementation).  $C_6$ ,  $C_7$ , and  $C_8$  represent the weights given to the three scores they precede. The sum of  $C_5$  through  $C_8$  should be lower than or equal to 1.

Blending edge filtering with edge interest scores is not trivial. If edge filtering scores are simply multiplied to the interest scores, then a user tracing a long edge may find that the edge disappears while his gaze reaches the edge mid-point. Thus, viewed edges should be “exempt” from filtering. To achieve this, the computed alpha values combine two components: what happens when edges are not filtered (the first term

in the summation) and what happens when they are filtered (the second term in the summation). Thus, for short term alphas (Alpha), in the case of non-filtered edges we combine a base component ( $C9$ ) with a component determined by ( $S_{ev,short}$ ) ( $C9 + C10 \leq 1$ ). The long-term alpha (Alpha') does not have a base component and thus this layer is invisible for edges that are not of interest.  $C12$  and  $C13$  are weights of the two scores they precede ( $C12 + C13 \leq 1$ ). Finally,  $C11$  and  $C14$  indicate the visibility of edges that should be filtered out but are currently viewed.

### 3.3. Implementation Notes

Our gaze correction implementation relies on fixations provided by the eye-tracking API. These fixations are computed by the API from a stream of gaze-samples acquired at a frequency of 120Hz. As such, they represent a discretization of the actual data stream. Conversely, the gaze interactions described in section 3.2 work directly with individual gaze samples. These small but frequent bits of information are aggregated over different time scales to indicate whether nodes and edges are being viewed. The advantage of this continuous approach over using discrete fixations is that responses can be gradual rather than binary, that errors are smaller and less noticeable, and that visual responses can be produced while a fixation is in progress.

All distance thresholds involved in gaze-based interactions should be defined in screen space. Whenever computations are done in visualization space, these thresholds need to be adjusted by the zoom level. For instance, the 500 pixel normalization threshold mentioned in section 3.2.2 refers to lengths on the screen rather than lengths in visualization space and conversions should be applied whenever necessary. Thus, since bar lengths are computed in model space we lower the 500 pixel threshold by a factor proportional to the zoom level.

## 4. Evaluation

### 4.1. Study design

We performed a within-subjects user study to evaluate our gaze-enabled network visualization (eye-tracking condition) against the same visualization without gaze interaction (control condition). The dataset used for the study was a book recommendation network dataset. The network had approximately 900 nodes and 2500 edges and had been drawn using the *neato* algorithm [?]. The eye-tracker used in the study was a RED120HZ from Sensory Motor Instruments (SMI).

We recruited 12 participants, 9 male and 3 female,

most of which were graduate students in our department. Their ages ranged between 24 and 30 years. None of the participants reported vision deficiencies or color blindness. Reimbursement was set at \$10 with an additional \$5 awarded to the user with the best aggregated accuracy over all tasks and conditions. The study lasted approximately one hour.

The study was designed to test the potential of gaze interactions to improve network tasks and to demonstrate the effectiveness of the gaze correction algorithm. For the first goal we tested two network tasks: determining the existence of direct connections (task 1) and finding shortest paths (task 2) between pairs of highlighted nodes, in the two conditions.

Instances of task 1 were limited at 3 seconds after which the screen faded out. Users would advance to the next question by pressing Y or N to answer the current question. We showed 175 instances of task 1, the same ones in both conditions. Users were not allowed to use the mouse.

Instances of task 2 were limited at 35 seconds and generally involved paths of length three or four. To provide their answers, users had to click on the nodes forming the path. Within the last five seconds of the total 35, the screen faded slightly indicating to users that time draws to an end and they should provide the answer. We showed 20 such questions, the same ones in both conditions. In this task users were allowed to pan but not zoom.

Users performed both tasks in one condition before solving them again in the other condition. To reduce learning effects, half of the participants started the study in the eye-tracking condition while the other half started with the control condition. A three minute break was introduced between the two conditions.

In a second stage we tested the effectiveness of the gaze-correction algorithm. With eye-tracking support enabled, users were shown a view of the graph in which a quarter of the nodes (225) were un-selected (gray) while all others were selected (red). They were then asked to select as many unselected nodes as possible in a two minute period by looking at them. They were allowed two minutes with gaze correction active and two minutes with gaze correction inactive. These two conditions were again alternated to minimize learning effects. In this task users could pan but not zoom.

The actual study was preceded by a training session. First, subjects were familiarized with the concepts of node-link diagrams and the tasks they were going to complete. They were then shown the visualization, several instances of tasks, and were instructed on how to advance through the study. For the first two tasks they were shown correct answers. Users were also

explained and shown how the gaze-enabled visualization reacts to their view.

Finally, at the end of the study subjects completed a short questionnaire indicating their preference between eye-tracking and conventional visualization, a 1 – 5 rating of the appeal and usefulness of eye-tracking, and a 1 – 5 indicator of whether the visual responses were obtrusive or not.

## 4.2. Results

Table 1 and Figure 8 list and summarize the quantitative results of our user study. We analyzed the data using a paired t-test and found statistically significant accuracy improvements in task 1 of approximately 30% and in task 3 of approximately 25%. No difference was found for task 2. The full results are listed below:

**task 1:**  $t(11) = 2.6719$ ,  $p = 0.02172$ , mean-difference= 12.5, effect size (Cohen’s d) = 0.7713;

**task 2:**  $t(11) = 0.745$ ,  $p = 0.4719$ , mean-difference= 0.5833, effect size (Cohen’s d) = 0.2151;

**task 3:**  $t(11) = 3.1017$ ,  $p = 0.01007$ , mean-difference= 14.17, effect size (Cohen’s d) = 0.8954.

In terms of qualitative assessment, all users expressed a preference for the eye-tracking enabled system, all of them rated it as helpful or very helpful, and most of them rated it as appealing or very appealing. These results are summarized in Figure 8. While not listed, none of the users found eye-tracking to be obtrusive.

We believe several reasons contributed to the lack of meaningful results for task 2. First of all, the high error rate (more than 50%) indicates that the task was difficult to complete within the allotted time. This is likely to have introduced significant variability in the results and made them highly depend on chance. Second, while striving to minimize obtrusiveness we may have reduced the visual effect to the point that it was no longer helpful. Finally, the technique itself works better in some case than others. For example, in highly connected networks, entire regions light up around viewed nodes, thereby rendering any highlighting advantage void. Additional research is required to improve this type of interaction.

An important result is that gaze correction was shown to be working. However, the magnitude of the improvement is dependent on factors such as eye-tracking calibration, lighting, or user particularities. In ideal settings, when eye-tracking works well, the correction effect would be negligible, such as in the case of users 5 and 7. In poor conditions the effect can be significant. For example, just two users performed better on task 1 in the control condition, users 2 and 8.

Those users also happen to have two of the most significant improvements in task 3, suggesting that the eye-tracking was not functioning properly. Conversely, users that show only mild improvements in task 3 generally showed significant improvements in task 1.

## 5. Discussion

Data visualization provides an ideal application area for eye-tracking enabled interactions because of the inherent interplays between eyes and visualization and between people’s gazes and tasks they are performing [YR67]. Current visualizations can be thought of as complete views that support many possible visual queries and tasks at the same time without specifically tending to any one of them. By interpreting users’ intentions from eye-tracking data, we can reduce perceptual overload and fit visualizations to user’s tasks and intentions, we reduce the overhead of manual interaction, and ultimately create visualization systems that participate proactively in the analytic process.

The results of our user study demonstrated the effectiveness of eye-tracking in supporting low level tasks but at the same time failed to reveal benefits in the more high-level task of path detection. We believe this was in part due to the design of our methods but also due to the difficulty of evaluating complex tasks quantitatively. However, given the reliability in detecting viewed nodes and edges, the strong effects in the short perceptual task, and the effectiveness of our gaze correction, we hypothesize that our methods can be used as a foundation for further exploration of high level interactive and analytic metaphors.

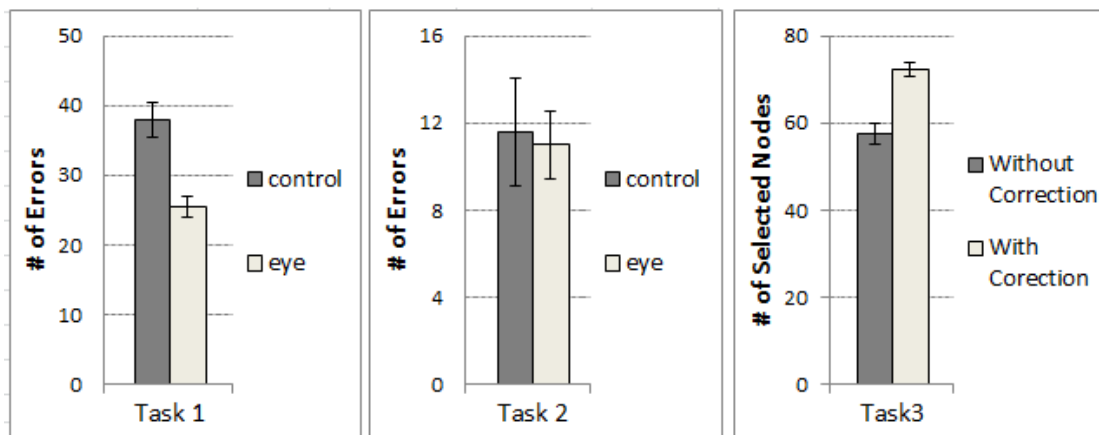
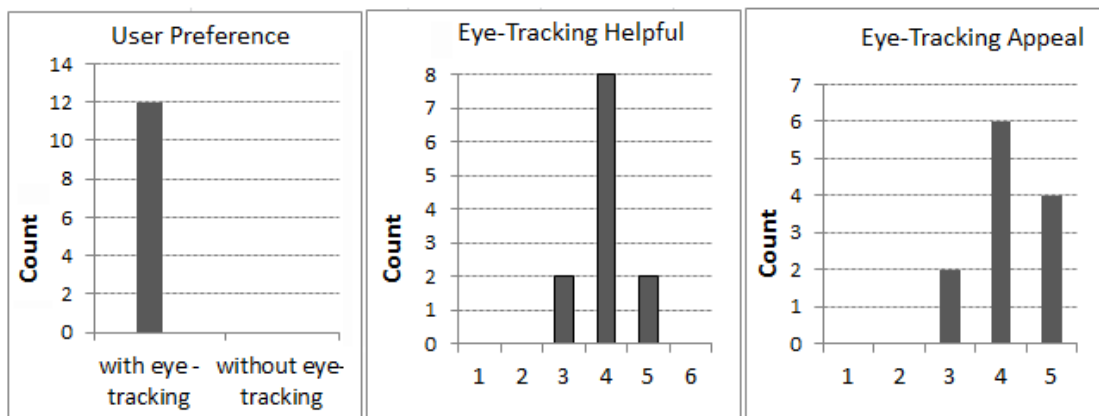
We also hypothesize that we can further improve on our detection of visual targets and user tasks. In sections 3.1 and 3.2.2 we mentioned several assumptions about peoples gaze patterns: long fixations for nodes, shorter fixations for edge (section 3.1); longer fixations in regions of high density, shorter fixations in regions of low density (section 3.2.2). These assumptions were made from informal observations during design and do not rely on data or models of visual perception. While such gaze models exist for specific areas such as reading, they have not been generalized for visual objects and layouts specific to our field. A better understanding of how visual parameters correlate to gaze measures such as fixation duration, saccade distance, or revisitation would enable us to detect viewed object in a more principled way.

In a complete analysis system additional information could be leveraged. For instance, since eye-movement and fixation precedes motor movement and action [Duc07], mouse patterns can be used to confirm and adjust data about fixations. Using our gaze-correction in an environment with multiple views, one



**Table 1:** Quantitative results.

Users	Eye-tracker first(y/n)	Task1-no-ET (#Errors)	Task1-ET (#Errors)	Task2-no-ET (#Errors)	Task2-ET (#Errors)	Task3-no GC (#Selected)	Task3-GC (#Selected)
user1	N	32	11	10	7	56	66
user2	N	16	20	10	8	17	59
user3	Y	32	19	12	8	103	85
user4	N	43	26	15	14	56	82
user5	Y	20	13	10	10	90	98
user6	N	47	46	15	15	63	64
user7	Y	80	23	11	12	81	87
user8	Y	43	49	13	13	20	49
user9	Y	34	24	7	12	63	77
user10	N	29	22	15	10	91	105
user11	N	51	37	10	12	41	71
user12	Y	29	16	11	11	41	49
Mean		38.0000	25.5000	11.5833	11.0000	60.1667	74.3333

**Figure 7:** Quantitative results.**Figure 8:** Qualitative user feedback.

visualization could correct offsets for another visualization that may occupy the same screen space.

Modeling of higher level analytic tasks specific to data visualization would allow us to apply similar principles to detecting and supporting tasks that go beyond perception and data reading. Gaze-enabled interactions can be explored at multiple temporal scales. Our methods hint at this by describing a perceptual task that is supported within a fraction of a second, and a deliberative task supported by visual responses spanning multiple seconds. Interactions that rely on data captured and aggregated during an entire analysis session or even extended periods of time would be worth exploring.

Finally, our work doesn't investigate the interplay between mouse interaction and gaze-interaction. A valid assumption is that users could outperform the eye-tracking enabled visualization in task 1 if allowed to select nodes and highlight their outgoing edges. In fact, one of the reasons for limiting task 1 to three seconds was our desire to capture the effect of eye-tracking on short, perceptual tasks for which the cost of interaction plays a significant overhead. We hypothesize that there is a class of interactive queries that would be cumbersome to specify manually and deliberately but would be easy to compute based on users' unconscious gaze patterns. Task 2 tried to capture such a query. Asking the user to provide and continuously update information about nodes of interest would be unfeasible. Using eye-tracking, the same process can be done automatically and without missing any of the user's visual interests.

## 6. Conclusion

In this paper we introduced techniques for using eye-tracking as an interactive input in the context of network visualization, and demonstrated their effectiveness in a controlled user study. Specifically, we dim out edges with endpoints outside of the users view focus, we highlight edges that are visually traced, and increase the saliency of sub-networks around nodes viewed often. We also describe an algorithm that improves eye-tracking accuracy by leveraging the known layout of the network. In a user study with twelve participants we showed that these techniques allow users to more accurately determine if two nodes are connected. At the same time we demonstrated the effectiveness of the gaze correction technique quantitatively. Given the reliability in detecting viewed nodes and edges, the strong effects in the connectivity task, and the success of the gaze correction technique, and the inherent role that eyes are playing in data visualization, we hypothesize that further exploration

of gaze-enabled interactions for visualization will be valuable.

## References

- [ADS05] ASHMORE M., DUCHOWSKI A. T., SHOEMAKER G.: Efficient eye pointing with a fisheye lens. In *Proceedings of Graphics interface 2005* (2005), Canadian Human-Computer Communications Society, pp. 203–210. **2**
- [BMBL09] BORGATTI S. P., MEHRA A., BRASS D. J., LABIANCA G.: Network analysis in the social sciences. *science* *323*, 5916 (2009), 892–895. **1**
- [BS09] BULLMORE E., SPORNS O.: Complex brain networks: graph theoretical analysis of structural and functional systems. *Nature Reviews Neuroscience* *10*, 3 (2009), 186–198. **1**
- [CCNS08] CHIN G., CHAVARRIA D., NAKAMURA G., SOFIA H.: Biographe: high-performance bionetwork analysis using the biological graph environment. *BMC bioinformatics* *9*, Suppl 6 (2008), S6. **1**
- [CGM04] COFFMAN T., GREENBLATT S., MARCUS S.: Graph-based technologies for intelligence analysis. *Communications of the ACM* *47*, 3 (2004), 45–47. **1**
- [DÇ07] DUCHOWSKI A. T., ÇÖLTEKIN A.: Foveated gaze-contingent displays for peripheral lod management, 3d visualization, and stereo imaging. *ACM Transactions on Multimedia Computing, Communications, and Applications (TOMCCAP)* *3*, 4 (2007), 6. **2**
- [DDL07] DREWES H., DE LUCA A., SCHMIDT A.: Eye-gaze interaction for mobile phones. In *Proceedings of the 4th international conference on mobile technology, applications, and systems and the 1st international symposium on Computer human interaction in mobile technology* (2007), ACM, pp. 364–371. **3**
- [DS07] DREWES H., SCHMIDT A.: Interacting with the computer using gaze gestures. In *Human-Computer Interaction—INTERACT 2007*. Springer, 2007, pp. 475–488. **3**
- [Duc02] DUCHOWSKI A. T.: A breadth-first survey of eye-tracking applications. *Behavior Research Methods, Instruments, & Computers* *34*, 4 (2002), 455–470. **1**
- [Duc07] DUCHOWSKI A. T.: *Eye tracking methodology: Theory and practice*, vol. 373. Springer, 2007. **2, 7**
- [GN00] GANSNER E. R., NORTH S. C.: An open graph visualization system and its applications to software engineering. *Software Practice and Experience* *30*, 11 (2000), 1203–1233. **1**
- [HDO03] HOWLETT S., DINGLIANA J. L., O'SULLIVAN C. A.: Eye movements and interactive graphics. **2**
- [HEH08] HUANG W., EADES P., HONG S.-H.: Beyond time and error: a cognitive approach to the evaluation of graph drawings. In *Proceedings of the 2008 Workshop on BEyond time and errors: novel evaluation methods for Information Visualization* (2008), ACM, p. 3. **2**
- [HMR05] HYRSKYKARI A., MAJARANTA P., RÄIHÄ K.-J.: From gaze control to attentive interfaces. In *Proceedings of HCI* (2005). **2**
- [Jac90] JACOB R. J.: What you look at is what you get:

- eye movement-based interaction techniques. In *Proceedings of the SIGCHI conference on Human factors in computing systems* (1990), ACM, pp. 11–18. [2](#)
- [Jac91] JACOB R. J.: The use of eye movements in human-computer interaction techniques: what you look at is what you get. *ACM Transactions on Information Systems (TOIS)* 9, 2 (1991), 152–169. [2](#)
- [JK03] JACOB R. J., KARN K. S.: Eye tracking in human-computer interaction and usability research: Ready to deliver the promises. *Mind* 2, 3 (2003), 4. [2](#)
- [KPW07] KUMAR M., PAEPCKE A., WINOGRAD T.: Eye-point: practical pointing and selection using gaze and keyboard. In *Proceedings of the SIGCHI conference on Human factors in computing systems* (2007), ACM, pp. 421–430. [2](#)
- [KT06] KURANT M., THIRAN P.: Extraction and analysis of traffic and topologies of transportation networks. *Physical Review E* 74, 3 (2006), 036114. [1](#)
- [LBP06] LI D., BABCOCK J., PARKHURST D. J.: openeyes: a low-cost head-mounted eye-tracking solution. In *Proceedings of the 2006 symposium on Eye tracking research & applications* (2006), ACM, pp. 95–100. [2](#)
- [MMC\*00] MAGLIO P. P., MATLOCK T., CAMPBELL C. S., ZHAI S., SMITH B. A.: Gaze and speech in attentive user interfaces. In *Advances in Multimodal Interfaces ICMI 2000*. Springer, 2000, pp. 1–7. [2](#)
- [MZ08] MACKENZIE I. S., ZHANG X.: Eye typing using word and letter prediction and a fixation algorithm. In *Proceedings of the 2008 symposium on Eye tracking research & applications* (2008), ACM, pp. 55–58. [3](#)
- [OHM\*04] OSULLIVAN C., HOWLETT S., MORVAN Y., McDONNELL R., O’CONNOR K.: Perceptually adaptive graphics. *Eurographics state of the art reports* 4 (2004). [2](#)
- [Ovi03] OVIATT S.: Multimodal interfaces. *The human-computer interaction handbook: Fundamentals, evolving technologies and emerging applications* (2003), 286–304. [1](#)
- [PSD09] POHL M., SCHMITT M., DIEHL S.: Comparing the readability of graph layouts using eyetracking and task-oriented analysis. In *Proceedings of the Fifth Eurographics conference on Computational Aesthetics in Graphics, Visualization and Imaging* (2009), Eurographics Association, pp. 49–56. [2](#)
- [RHN\*03] RUDDARRAJU R., HARO A., NAGEL K., TRAN Q. T., ESSA I. A., ABOWD G., MYNATT E. D.: Perceptual user interfaces using vision-based eye tracking. In *Proceedings of the 5th international conference on Multimodal interfaces* (2003), ACM, pp. 227–233. [2](#)
- [SA00] SALVUCCI D. D., ANDERSON J. R.: Intelligent gaze-added interfaces. In *Proceedings of the SIGCHI conference on Human factors in computing systems* (2000), ACM, pp. 273–280. [3](#)
- [Sal99] SALVUCCI D. D.: Inferring intent in eye-based interfaces: tracing eye movements with process models. In *Proceedings of the SIGCHI conference on Human Factors in Computing Systems* (1999), ACM, pp. 254–261. [3](#)
- [Sel04] SELKER T.: Visual attentive interfaces. *BT Technology Journal* 22, 4 (2004), 146–150. [1](#)
- [TJ00] TANRIVERDI V., JACOB R. J.: Interacting with eye movements in virtual environments. In *Proceedings of the SIGCHI conference on Human factors in computing systems* (2000), ACM, pp. 265–272. [2](#)
- [Ver02] VERTEGAAL R.: Designing attentive interfaces. In *Proceedings of the 2002 symposium on Eye tracking research & applications* (2002), ACM, pp. 23–30. [2](#)
- [VS08] VERTEGAAL R., SHELL J. S.: Attentive user interfaces: the surveillance and sousveillance of gaze-aware objects. *Social Science Information* 47, 3 (2008), 275–298. [2](#)
- [VSCM06] VERTEGAAL R., SHELL J. S., CHEN D., MAMUJI A.: Designing for augmented attention: Towards a framework for attentive user interfaces. *Computers in Human Behavior* 22, 4 (2006), 771–789. [2](#)
- [WM87] WARE C., MIKAELEIAN H. H.: An evaluation of an eye tracker as a device for computer input2. In *ACM SIGCHI Bulletin* (1987), vol. 17, ACM, pp. 183–188. [2](#)
- [YR67] YARBUS A. L., RIGGS L. A.: *Eye movements and vision*, vol. 2. Plenum press New York, 1967. [2](#), [7](#)
- [ZMI99] ZHAI S., MORIMOTO C., IHDE S.: Manual and gaze input cascaded (magic) pointing. In *Proceedings of the SIGCHI conference on Human factors in computing systems* (1999), ACM, pp. 246–253. [1](#), [2](#)